

Revealing the nature of nonequilibrium phase transitions with quantum trajectories

Valentin Link,^{*} Kimmo Luoma,[†] and Walter T. Strunz[‡]

Institut für Theoretische Physik, Technische Universität Dresden, D-01062 Dresden, Germany



(Received 5 December 2018; published 26 June 2019)

A damped and driven collective spin system is analyzed by using quantum state diffusion. This approach allows for a mostly analytical treatment of the investigated nonequilibrium quantum many-body dynamics, which features a phase transition in the thermodynamical limit. The exact results obtained in this work, which are free of any finite-size defects, provide a complete understanding of the model. Moreover, the trajectory framework gives an intuitive picture of the two phases occurring, revealing a spontaneously broken symmetry and allowing for a qualitative and quantitative characterization of the phases. We determine exact critical exponents, investigate finite-size scaling, and explain a remarkable nonalgebraic behavior at the transition in terms of torus hopping.

DOI: [10.1103/PhysRevA.99.062120](https://doi.org/10.1103/PhysRevA.99.062120)

I. INTRODUCTION

Many important models from the early years of quantum optics, like the Dicke model [1], have experienced renewed interest, the reason being the availability of new experimental platforms. First and foremost, the field of ultracold atomic gases allows an unprecedented level of control and tunability, bringing relatively simple but physically rich quantum optical models within the reach of current state of the art experiments [2–5]. The Dicke model, for example, can be realized for a wide range of parameters covering different phases of the system [6,7]. Similar models are studied in the context of quantum magnetism [8–10]. Experiments are often performed under interesting nonequilibrium conditions where the interplay of driving and dissipation determines a stationary state of the system in the absence of detailed balance [11–13]. The dissipation stems from interactions with an environment which in many cases cannot be avoided. If the driven open system exhibits a phase transition upon tuning the system parameters, the nonequilibrium stationary state, rather than the ground state of the Hamiltonian, undergoes a nonanalytical change. This poses a formidable challenge for the theoretical treatment of such a system. The understanding of phase transitions in driven dissipative quantum many-body systems is still developing [14–16], as such problems, in general, can be tackled only approximately [17].

Analytically soluble models containing the relevant physics are highly desirable and of great value for exploring in great detail new phenomena arising in this field. A recent trend has been to describe driven dissipative systems in the language of nonequilibrium quantum field theory [3,11]. There, a path-integral formalism for Gorini-Kossakowski-Sudarshan-Lindblad (GKSL) master equations [18], conceptually similar to the Keldysh functional integrals, are used [11]. Such path-

integral representations of dissipative propagators were earlier studied in a quantum optics setting in [19].

Alternatively, quantum trajectory methods from the field of quantum optics [20,21], such as quantum state diffusion [20], also provide an efficient and transparent theoretical framework. They can contribute to a detailed understanding of nonequilibrium quantum physics, as we will demonstrate in this article. In particular, the localization property of quantum state diffusion in the long-time limit [22] is useful for the qualitative and quantitative analysis of nonequilibrium phase transitions, since this allows a direct observation of the different character of distinct phases. Quantum trajectories have been used successfully in [4] to analyze a generalization of the Dicke model. In the present article we consider a model similar to the so-called cooperative resonance fluorescence model introduced in the 1970s [23–25]. The latter recently received attention because it features a particularly interesting phase transition which is difficult to characterize [14,26]. We here show that our model can be treated exactly within a quantum trajectory approach. This gives a clear picture of the different phases, helps to identify a broken symmetry, allows for an analytical, rather than numerical, determination of critical exponents, and explains the peculiar critical behavior. For the sake of readability and providing insight to the physics rather than to technical aspects, we postpone detailed derivations to the Appendix, while keeping the main text self-contained.

II. MODEL

We consider the following master equation of GKSL form [18] for a driven damped spin- j system:

$$\begin{aligned} \partial_t \rho = & -i\omega[J_x, \rho] + \frac{\kappa}{j} \left(J_+ \rho J_- - \frac{1}{2} \{J_- J_+, \rho\} \right) \\ & + \frac{\kappa}{j} \left(J_z \rho J_z - \frac{1}{2} \{J_z^2, \rho\} \right), \end{aligned} \quad (1)$$

where J_z , $J_{\pm} = J_x \pm iJ_y$ are the spin operators. Apart from the additional J_z dissipator this coincides with the cooperative resonance fluorescence model [23–25,27,28]. It can describe

^{*}valentin.link@tu-dresden.de

[†]kimmo.luoma@tu-dresden.de

[‡]walter.strunz@tu-dresden.de

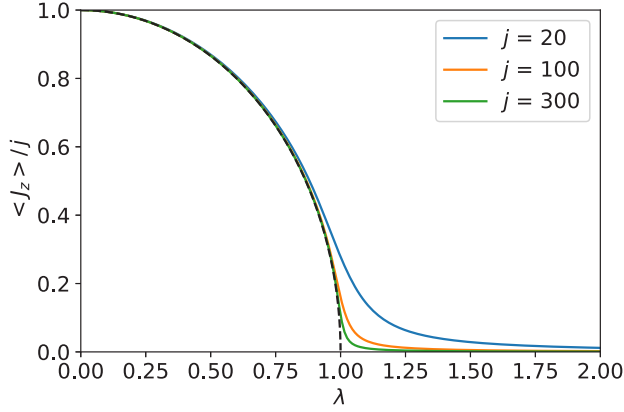


FIG. 1. J_z expectation value in the steady state of master equation (1) as a function of the parameter λ for different values of j . The dashed line is the asymptotic curve for $j \rightarrow \infty$ from (9).

j spin- $\frac{1}{2}$ systems undergoing collective driving and collective damping. Following the proposals in [14,26] this model could be realized experimentally with cold atoms. Interestingly, in theoretical models for engineered atomic spin devices used to describe tunneling spectroscopy of atomic magnets on metallic surfaces, a similar GKSL dissipator appears naturally [8–10]. A phase diagram of this model was examined in [9]. Recently also the stability of the peculiar properties of this model in the presence of noncollective decay [29] and many-body correlations [30] have been discussed.

The stationary state of (1) features a phase transition in the thermodynamic limit $j \rightarrow \infty$ as the parameter $\lambda = \frac{\omega}{\kappa}$, measuring the relative strength of coherent drive to dissipation, is changed. For strong damping $\lambda < 1$ the steady state has a finite J_z expectation value. If instead $\lambda > 1$ the J_z expectation value is zero; see Fig. 1.

It is important to stress that Eq. (1) has a discrete symmetry. It is invariant under mirror reflection given by $J_x \rightarrow -J_x$ followed by complex conjugation. The crucial role of this symmetry for the phase transition becomes apparent when we add a symmetry-breaking term of the form $\omega_z J_z$ to the Hamiltonian. As shown in the Appendix, the model then features only a first-order transition.

III. QUANTUM STATE DIFFUSION APPROACH

We analyze the model (1) by unraveling the master equation with quantum state diffusion; that is, we express the density operator ρ as the average over stochastic pure states [20,21]. In contrast to the cooperative resonance fluorescence model, due to the additional J_z dissipator, the resulting stochastic Schrödinger equation preserves spin coherent states for *any* j , that is, for any system size [31]. The spin coherent states are defined as

$$|\mu\rangle = \frac{||\mu\rangle}{\sqrt{\langle\mu||\mu\rangle}}, \quad ||\mu\rangle = \exp(\mu J_-) |j\rangle, \quad (2)$$

and the density operator is obtained by averaging over the stochastically evolving spin coherent states $\rho(t) = \mathbb{E}(|\mu(t)\rangle\langle\mu(t)|)$ where the complex labels $\mu(t)$ are stochastic

trajectories obeying the classical Langevin equation

$$d\mu = \left(-i\frac{\omega}{2}(1 - \mu^2) - \tilde{\kappa}\mu \right) dt + \sqrt{\frac{\kappa}{j}}\mu^2 d\xi_+ - \sqrt{\frac{\kappa}{j}}\mu d\xi_z, \quad (3)$$

with complex Ito increments $\mathbb{E}(d\xi_\alpha) = 0$ and $d\xi_\alpha d\xi_\beta^* = \delta_{\alpha\beta} dt$. See the Appendix for the derivation of (3). A rescaled coupling is introduced as $\tilde{\kappa} = \kappa(1 + \frac{1}{2j})$. That spin coherent states are preserved is remarkable [31], and reflects the localization property of quantum state diffusion [22]. It allows one to solve this model particularly easily. Nevertheless, in the following we see that this model features qualitatively the same physics as the cooperative resonance fluorescence model. Unlike mean-field or semiclassical approaches, Eq. (3) provides the exact solution of the master equation (1) for any system size.

IV. SOLUTION IN THE THERMODYNAMIC LIMIT

Neglecting the noise terms in Eq. (3) results in the deterministic equation

$$\dot{\mu} = -i\frac{\omega}{2}(1 - \mu^2) - \tilde{\kappa}\mu. \quad (4)$$

Since the strength of fluctuations is κ/j this is valid for times much smaller than j/κ . In particular, it captures the thermodynamic limit $j \rightarrow \infty$. The resulting approximate solutions of Eq. (1) are coherent states with deterministic label μ obeying Eq. (4). These pure states are just the so-called robust states of the master equation [32]. At this point we already note that for *any* finite j the asymptotic state $\rho(t = \infty)$ of Eq. (1) may nevertheless be highly mixed, as will be further elaborated later.

The solution of Eq. (4) can be found analytically

$$\mu_{\mathcal{M}}(t) = \frac{\mu_- \sqrt{1 + \mathcal{M}} e^{i\phi(t)} - \mu_+ \sqrt{1 - \mathcal{M}}}{\sqrt{1 + \mathcal{M}} e^{i\phi(t)} - \sqrt{1 - \mathcal{M}}}, \quad (5)$$

with the phase $\phi(t) = \sqrt{\lambda^2 - 1}\tilde{\kappa}t + \phi(0)$. \mathcal{M} ($|\mathcal{M}| \leq 1$) and $\phi(0)$ are determined by the initial condition. There are two fixed points

$$\mu_{\pm} = -i\frac{\tilde{\kappa}}{\omega}(1 \pm \sqrt{1 - \lambda^2}) \quad (6)$$

corresponding to $\mathcal{M} = \pm 1$. The most elegant way of displaying the trajectories is to map the complex label μ to a point on the sphere via the inverse stereographic projection given by

$$\vec{n} = \langle \mu | \vec{J} | \mu \rangle / j. \quad (7)$$

Some of the deterministic trajectories are depicted in Fig. 2 for two values of λ . For $\lambda < 1$ all trajectories flow to the stable fixed point μ_- . In contrast, the solutions are periodic for $\lambda > 1$, i.e., $\mu_{\mathcal{M}}(t)$ traverses a closed torus with period $T = 2\pi(\tilde{\kappa}\sqrt{\lambda^2 - 1})^{-1}$. As a consequence of the existence of periodic solutions, the spectrum of the Lindbladian becomes gapless and the imaginary parts of the eigenvalues are separated by the fundamental frequency $2\pi/T$, as observed in [26]. Clearly, the existence of two distinct phases in the thermodynamic limit is evident. In the case $\lambda < 1$ there is a unique stable (unstable) steady state which is the coherent state $\rho_- = |\mu_- \rangle \langle \mu_- |$ ($\rho_+ = |\mu_+ \rangle \langle \mu_+ |$). For $\lambda > 1$ a steady

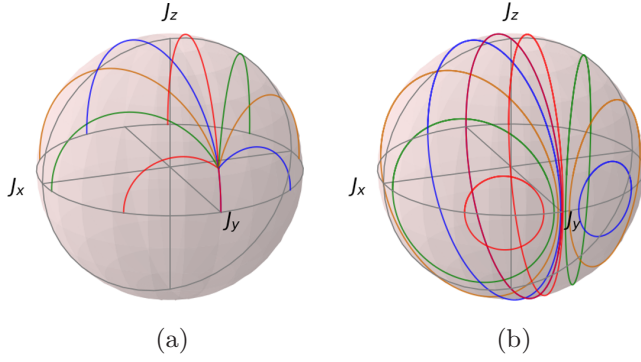


FIG. 2. Deterministic trajectories Eq. (4) displayed on the sphere with initial conditions on the equator. In case (a) ($\lambda = 0.95$) all trajectories flow to a stable fixed point. In case (b) ($\lambda = 1.05$) solutions are cyclic.

state can be associated with each torus labeled with \mathcal{M} , by time averaging the cyclic evolution over one period:

$$\rho_{\mathcal{M}} = \frac{1}{T} \int_0^T dt |\mu_{\mathcal{M}}(t)\rangle \langle \mu_{\mathcal{M}}(t)|. \quad (8)$$

The emergence of periodic solutions has led to the idea that such a phase transition can be associated with a spontaneous breaking of continuous-time translation symmetry [26]. Here, however, we can clearly see that the mirror symmetry of the Lindblad generator (1) is spontaneously broken in the $\lambda > 1$ phase. The steady states $\rho_{\mathcal{M}}$ in Eq. (8) are not mirror symmetric, since the mirrored state is $\rho_{-\mathcal{M}}$ [33]. Thus the phase transition happens in the presence of an ordinary symmetry breaking [9]. Note that all steady states $\rho_{\mathcal{M}}$ have a vanishing J_z expectation value and thus the steady-state value of J_z is well defined:

$$\frac{\langle J_z \rangle}{j} = \begin{cases} \sqrt{1 - \lambda^2}, & \lambda < 1, \\ 0, & \lambda > 1, \end{cases} \quad (9)$$

indicating a second-order phase transition. When in the Hamiltonian an additional symmetry-breaking term $\omega_z J_z$ is present there are no cyclic solutions and a stable fixed point exists for all λ (see Appendix and Fig. 6). The system is then no longer critical at $\lambda = 1$.

V. FINITE SYSTEM SIZE

If the system has a finite size $j < \infty$ there always exists a unique steady state which is the asymptotic solution of (1). The uniqueness is seemingly at odds with the previous investigation in the thermodynamic limit, where for $\lambda > 1$ we found a whole family of steady states. The explanation goes as follows. Neglecting the noise terms, as we did in Eq. (4), is only valid for times much shorter than j/κ . On longer time scales the noise will lead to a mixing process which results in a unique steady state. In Fig. 3 two quantum trajectories are displayed in the two regimes. For $\lambda < 1$ there exists a stable fixed point and a weak ($1/j$) noise will only cause small fluctuations around this point; see Fig. 3(a). On the other hand, in the presence of cyclic solutions, when $\lambda > 1$, the noise introduces a hopping between neighboring tori; see Fig. 3(b).

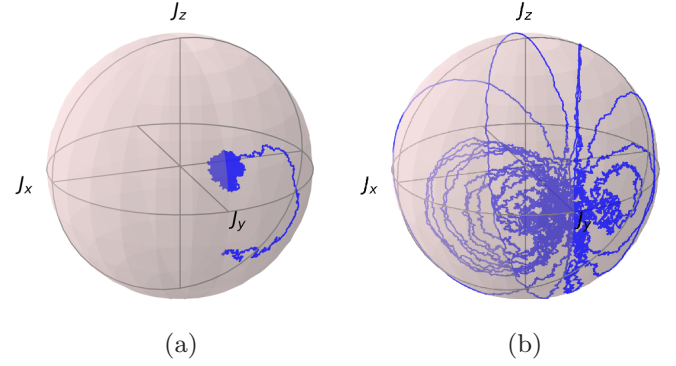


FIG. 3. Example of a noisy trajectory Eq. (3) for $j = 500$. At $\lambda = 0.95$ (a) a trajectory starting at the unstable fixed point evolves to the stable fixed point and remains there. At $\lambda = 1.05$ (b) a trajectory starting at the right fixed point hops stochastically between the deterministic tori depicted in Fig. 2(b), such that it eventually explores the entire phase space.

Torus hopping allows a single trajectory to eventually explore the entire phase space.

In Fig. 4(a) the J_z variance of the unique steady state is displayed for different values of j . Clearly, the variance increases with λ and for large system sizes approaches a curve which is nonanalytic at $\lambda = 1$. With the trajectories displayed in Fig. 3 this can be understood in an intuitive way. Moreover, we can even compute analytically the asymptotic curve displayed in Fig. 4(a). To this aim it is useful to switch to the “action-angle” variables (\mathcal{M}, ϕ) used for the deterministic trajectories (5). As elaborated in the Appendix, averaging over the fast dynamics of the angle variable [25,34,35] results in a one-dimensional stochastic evolution for the torus label \mathcal{M} , reflecting the slow torus-hopping process. A stationary distribution for this process can be found analytically:

$$P(\mathcal{M}) = \frac{1}{2} \frac{\sqrt{1 + 2\lambda^2}}{\tanh^{-1}((1 + 2\lambda^2)^{-1/2})} \frac{1}{2\lambda^2 + 1 - \mathcal{M}^2}. \quad (10)$$

The unique steady state resulting from the mixing induced by the torus hopping is

$$\rho_{ss} = \int_{-1}^1 d\mathcal{M} P(\mathcal{M}) \rho_{\mathcal{M}}, \quad (11)$$

with $\rho_{\mathcal{M}}$ from (8). Naturally, this unique state does have the same symmetries as the Lindblad generator, since $P(\mathcal{M})$ is a symmetric distribution. We note in passing that the additional J_z dissipator of the present model leads to a different distribution of tori compared to the one derived by Carmichael using a Glauber P -distribution technique in [34]. The J_z variance of ρ_{ss} can be given in closed form,

$$\frac{\Delta J_z^2}{j^2} = (\lambda^2 - 1) \left(\frac{\tanh^{-1}(\sqrt{3}(1 + 2\lambda^2)^{-1/2})}{\sqrt{3} \tanh^{-1}((1 + 2\lambda^2)^{-1/2})} - 1 \right), \quad (12)$$

displayed as the dashed line in Fig. 4(a). Interestingly, this function does not behave like a power law for λ close to one. With $\lambda = 1 + \varepsilon$ we find that the asymptotic curve behaves as $-\varepsilon \ln \varepsilon$. This behavior is hard to find from extrapolating finite-size calculations, as can be seen in Fig. 4(b). There we plot “exponents” β that one would associate to the limiting

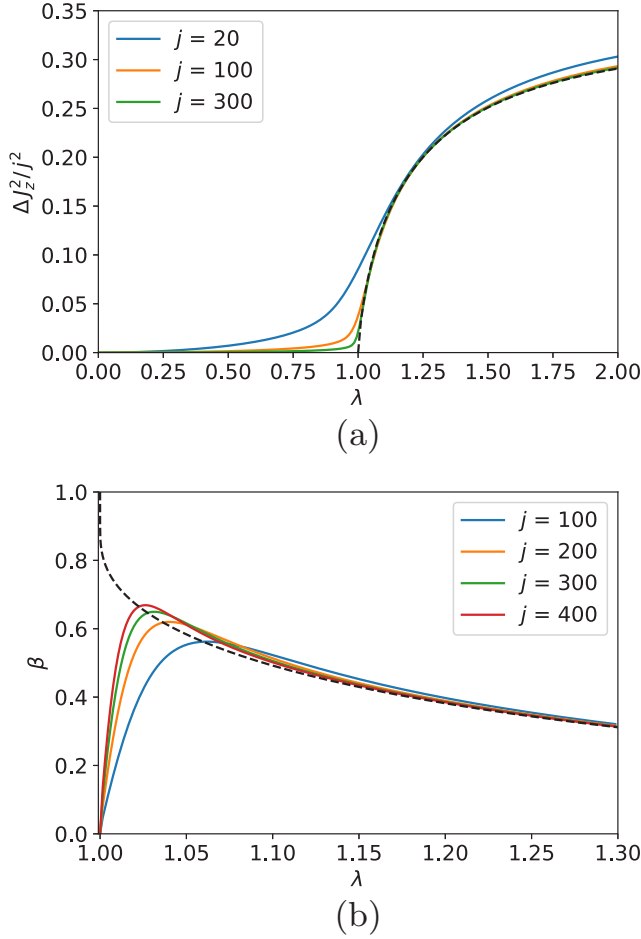


FIG. 4. Variance of J_z in the steady state of master equation (1) as a function of the parameter λ for different values of j (a). The dashed line is the asymptotic curve for large j from (12). Estimates for the power-law “exponent” β of the J_z variance are plotted in (b). The assignment of a critical exponent close to $\lambda = 1$ from finite system calculations fails because the asymptotic curve does not behave like a power law in the vicinity of the transition.

curve by assuming a power law, estimated for different values of $\lambda = 1 + \varepsilon$. Clearly we see from the exact curve that close to $\lambda = 1$ no exponent can be associated, and the peculiar behavior $\beta \simeq 1 + \frac{1}{\ln(\varepsilon)}$ with an infinite negative slope at the critical point follows.

In the thermodynamic limit different steady states (8) do not have the same J_z variance, and thus this quantity is not well defined. As a consequence, this observable does not have a universal power-law scaling close to the transition point—see the Appendix for more details. Figure 4(b) manifests also the noncommutativity of the two types of limiting procedures involved. The nonuniversal behavior is a finite system size effect which emerges when first the stationary state is found and only afterwards the limit of large system size is taken. In order to correctly understand the phase transition, the order of limits has to be interchanged. Neglecting the $1/j$ terms, as in (4), corresponds to first taking the strict thermodynamic limit leading to the family of steady states (8). Naively computing the steady state of (1) for finite j results always in a unique steady state and the broken symmetry is not revealed.

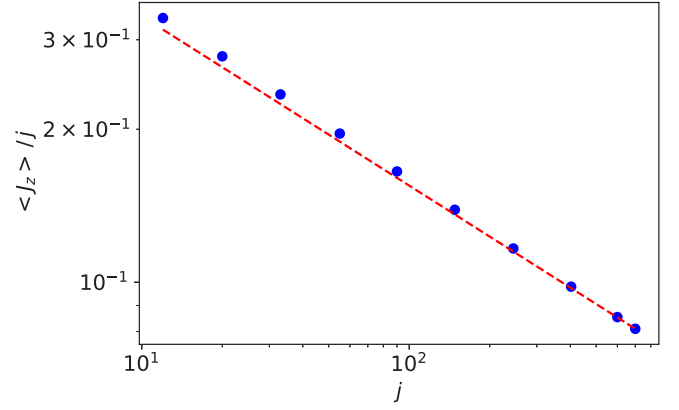


FIG. 5. J_z steady-state expectation value at $\lambda = 1$ for different values of j . The dashed line has the predicted slope $-1/3$.

VI. CRITICAL EXPONENTS AND FINITE-SIZE SCALING

Clearly, Eq. (9) gives the critical exponent $1/2$ for the J_z expectation value. From the exact solution in the thermodynamic limit (5) we can just as easily read off the dynamical critical exponent. Since there is only a single time scale $\xi = |1 - \lambda^2|^{-1/2} \kappa^{-1}$ the dynamical exponent is also $1/2$. With the exact Ito equations at hand it is also possible to find finite-size scaling exponents at $\lambda = 1$ by using a renormalization scheme as in [3,5]. Numerically we observe a finite-size power-law scaling at the transition point; see Fig. 5. To obtain the exponent analytically we set $v = \mu + i$ and the evolution equation (3) is rewritten as

$$dv = i \frac{\tilde{\kappa}}{2} v^2 dt + \sqrt{\frac{\kappa}{j}} (v - i) d\xi_z + \sqrt{\frac{\kappa}{j}} (v - i)^2 d\xi_+. \quad (13)$$

Under a rescaling of time, close to the transition, v has power-law scaling.

Indeed, the noiseless equation is invariant under the transformation

$$t \rightarrow at, \quad v \rightarrow \frac{v}{a}. \quad (14)$$

This transformation changes the evolution equation to [36]

$$dv = i \frac{\tilde{\kappa}}{2} v^2 dt + a^{3/2} \sqrt{\frac{\kappa}{j}} \left(\frac{v}{a} - i \right) d\xi_z + a^{3/2} \sqrt{\frac{\kappa}{j}} \left(\frac{v}{a} - i \right)^2 d\xi_+.$$

For the theory (with fluctuations) to be scale invariant at low frequencies, j must scale as [3,5]

$$\frac{\kappa}{j} \rightarrow \frac{1}{a^3} \frac{\kappa}{j}. \quad (15)$$

Then all noise terms containing v/a become irrelevant under renormalization and the resulting low-frequency theory with constant noise is scale invariant. The finite- j scaling of v is found to be $(\kappa/j)^{-1/3} v \sim 1$. With $\mu = v - i$, we conclude that for large j

$$\langle \mu | J_z | \mu \rangle / j \sim v + O(v^2) \approx v \sim \left(\frac{\kappa}{j} \right)^{1/3}. \quad (16)$$

As seen in Fig. 5, numerically accessible values match this law quite well.

VII. CONCLUSIONS

Quantum state diffusion for nonequilibrium quantum dynamics allows us to obtain exact analytical results for a driven dissipative many-body quantum system featuring a phase transition. We are able to identify the symmetries of the different phases emerging in the thermodynamical limit, and in this way we can reveal the symmetry breaking associated with the phase transition. For these findings the trajectory picture proves insightful. Moreover, it provides an elegant shortcut to an exact analytical treatment. The physics in the trajectory framework can be characterized by two time scales, T and j/κ , which describe the deterministic evolution of the open system and the fluctuations, respectively. In the thermodynamic limit ($j \rightarrow \infty$) the relaxation time scale is infinitely large and the system does not relax, resulting in the degeneracy of the stationary state. Even though we here consider a solvable model in terms of spin coherent states, quantum state diffusion trajectories would reveal the underlying character of the phases also for finite j and for nonlinear Hamiltonians. These results strongly support the idea that quantum trajectories help to unravel nonequilibrium phenomena in many-body quantum dynamics.

ACKNOWLEDGMENTS

It is a pleasure to thank Holger Kantz and Konrad Merkel for discussions and advice. V.L. acknowledges support from the International Max Planck Research School (IMPRS) of MIPPKS Dresden.

APPENDIX

1. Quantum state diffusion

Our starting point is the Gorini-Kossakowski-Sudarshan-Lindblad (GKSL) master equation (1) where, in addition to the master equation in the main text, we choose a more general Hamiltonian including a symmetry-breaking term $H = \omega J_x + \omega_z J_z$. In quantum state diffusion (QSD) the solution of a Lindblad master equation is expressed as an ensemble average over stochastic pure quantum states

$$\rho = \mathbb{E}(|\psi\rangle\langle\psi|), \quad (\text{A1})$$

where the pure states $|\psi_t\rangle$ are realizations of a stochastic process in Hilbert space determined from the nonlinear QSD equation [20]. For the present GKSL equation this reads

$$\begin{aligned} d|\psi\rangle = & -iH|\psi_t\rangle dt + \sqrt{\frac{\kappa}{j}}(J_+ - \langle J_+ \rangle)|\psi\rangle d\xi_+ \\ & - \frac{\kappa}{2j}(J_- J_+ - 2\langle J_- \rangle J_+ + \langle J_- \rangle \langle J_+ \rangle)|\psi\rangle dt \\ & + \sqrt{\frac{\kappa}{j}}(J_z - \langle J_z \rangle)|\psi\rangle d\xi_z - \frac{\kappa}{2j} \\ & \times (J_z^2 - 2\langle J_z \rangle J_z + \langle J_z \rangle \langle J_z \rangle)|\psi\rangle dt, \end{aligned} \quad (\text{A2})$$

with independent complex Ito-noise increments $d\xi_+$ and $d\xi_z$. The noise terms give rise to the average in (A1), with statistics $\mathbb{E}(d\xi_\alpha) = 0$, $\mathbb{E}(d\xi_\alpha d\xi_\alpha^*) = dt$, and $\mathbb{E}(d\xi_\alpha d\xi_\beta) = 0$. Brackets $\langle O \rangle \equiv \langle \psi_t | O | \psi_t \rangle$ denote expectation values with respect to the state $|\psi\rangle$ and make this equation nonlinear. Note that because of the symmetric combination of “damping” (J_+ terms) and “dephasing” (J_z terms) in the present case the equation can be simplified with the relation $J_- J_+ + J_z^2 = j(j+1) - J_z$. As a consequence, the QSD equation preserves coherent states, i.e., the equation is solved by a coherent state ansatz

$$|\psi\rangle = e^{i\phi} |\mu\rangle = N |\mu\rangle, \quad (\text{A3})$$

where N is a normalization [31]. We use a Bargmann-like complex parametrization of spin coherent states, which is handy for analytical computations but also appears rather formal. The coherent state “labels” μ can alternatively be expressed with spherical angles φ, θ given by

$$\cos\theta = \frac{1 - |\mu|^2}{1 + |\mu|^2}, \quad \varphi = \arg \mu, \quad (\text{A4})$$

which parametrize the expectation values of the spin operator as usual:

$$\langle \mu | \vec{J} | \mu \rangle = j \begin{pmatrix} \cos\varphi \sin\theta \\ \sin\varphi \sin\theta \\ \cos\theta \end{pmatrix}. \quad (\text{A5})$$

For convenience, we stick to the complex parametrization and provide the relations

$$\begin{aligned} J_z |\mu\rangle &= (j - \mu J_-) |\mu\rangle, \\ J_+ |\mu\rangle &= (2j\mu - \mu^2 J_-) |\mu\rangle, \\ J_- |\mu\rangle &= \partial_\mu |\mu\rangle. \end{aligned} \quad (\text{A6})$$

These can be employed upon inserting the coherent state ansatz in (A2). The left-hand side of (A2) becomes

$$d|\psi\rangle = \frac{dN}{N} |\psi\rangle + d\mu \partial_\mu |\psi\rangle.$$

Note that using the usual Itô rule one has to consider also second-order terms like $d\mu d\mu$. However, since $|\psi\rangle$ is a holomorphic functional of the stochastic processes $\xi_{\pm/z}$, these terms vanish by $d\xi_\alpha d\xi_\alpha = 0$. We can simply compare terms proportional to $\partial_\mu |\psi\rangle$ on the left- and right-hand side to find an equation for the label μ . After carrying out the computations the resulting equation is

$$d\mu = -i\frac{\omega}{2}(1 - \mu^2)dt + (i\omega_z - \tilde{\kappa})\mu dt \quad (\text{A7})$$

$$+ \sqrt{\frac{\kappa}{j}}\mu^2 d\xi_+ + \sqrt{\frac{\kappa}{j}}\mu d\xi_z, \quad (\text{A8})$$

with $\tilde{\kappa} = \kappa(1 + \frac{1}{2j})$. The QSD equation (A2) preserves the norm, and thus we have $|N|^2 = \langle \mu | \mu \rangle^{-1}$.

2. Analytical solution in the thermodynamic limit

In the thermodynamic limit $j \rightarrow \infty$ fluctuations can be neglected and we obtain the deterministic equation

$$\dot{\mu} = -i\frac{\omega}{2}(1 - \mu^2)dt + (i\omega_z - \tilde{\kappa})\mu$$

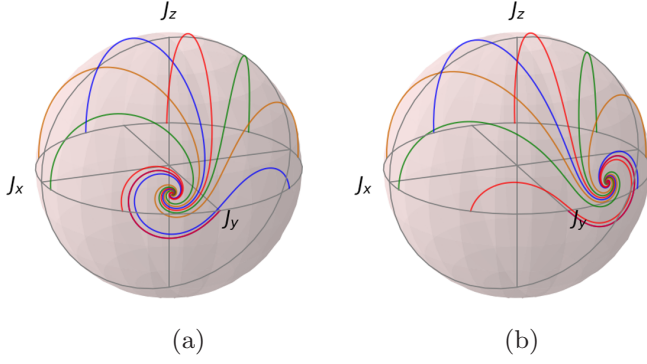


FIG. 6. Deterministic trajectories (A11) on the sphere with initial conditions on the equator, and for $\lambda = 1.05$. Unlike the $\omega_z = 0$ case displayed in Fig. 2(b), due to a symmetry breaking term, there exists a stable fixed point. (a) $\omega_z = 0.1\omega$; (b) $\omega_z = -0.1\omega$.

$$= i\frac{\omega}{2}(\mu - \mu_+)(\mu - \mu_-), \quad (\text{A9})$$

where μ_{\pm} denotes the two fixed points

$$\mu_{\pm} = \frac{-i}{\omega}((\tilde{\kappa} - i\omega_z) \pm \sqrt{(\tilde{\kappa} - i\omega_z)^2 - \omega^2}). \quad (\text{A10})$$

The general solution of this Riccati-type differential equation can easily be found by the standard mapping to a second-order linear equation. The explicit solution is

$$\mu_{\mathcal{M}}(t) = \frac{\sqrt{1+\mathcal{M}}e^{-\Omega t+i\phi_0}\mu_+ - \sqrt{1-\mathcal{M}}\mu_-}{\sqrt{1+\mathcal{M}}e^{-\Omega t+i\phi_0} - \sqrt{1-\mathcal{M}}}, \quad (\text{A11})$$

$$\Omega = \sqrt{(\tilde{\kappa} - i\omega_z)^2 - \omega^2},$$

with \mathcal{M} and ϕ_0 determined from the initial condition at $t = 0$. Whenever Ω has a nonvanishing real part there exists a stable fixed point, which is the steady state of the model. In the special case $\omega_z = 0$ and $\lambda = \frac{\omega}{\tilde{\kappa}} > 1$, Ω is purely imaginary and the solutions are cyclic. The constant \mathcal{M} , in this phase, has the simple expression

$$\mathcal{M} = \sqrt{\lambda^2 - 1} \frac{\text{Re}(\mu_{\mathcal{M}}(t))}{\text{Im}(\mu_{\mathcal{M}}(t)) - \frac{\lambda}{2}(1 + |\mu_{\mathcal{M}}(t)|^2)}, \quad (\text{A12})$$

and labels each invariant torus with a number in the interval $[-1, 1]$. Since the model lacks symmetry whenever $\omega_z \neq 0$, there can be no symmetry breaking and no continuous phase transitions occur. Note, however, that a first-order transition occurs for $\omega > \tilde{\kappa}$, upon changing ω_z from positive to negative; see Fig. 6.

3. Derivation of the unique steady state for finite system size

In this section we focus on the symmetry-breaking phase $\lambda > 1$ and $\omega_z = 0$. If the system size is finite, the noise terms in Eq. (A8) cannot be neglected. However, assuming a large j , the time scale $1/|\Omega|$ of the deterministic term is much faster than the time scale j/κ of the noise. This decoupling of time scales allows us to find an analytical expression for the stationary state. This scheme was also used by Drummond and Carmichael in [25,34], and Kruscha *et al.* [35]. Here we want to repeat their argument and provide the results for the present model. First we switch to the “action-angle coordinates” \mathcal{M}

and ϕ given by

$$\mu(\mathcal{M}, \phi) = \frac{\sqrt{1+\mathcal{M}}e^{i\phi}\mu_+ - \sqrt{1-\mathcal{M}}\mu_-}{\sqrt{1+\mathcal{M}}e^{i\phi} - \sqrt{1-\mathcal{M}}}. \quad (\text{A13})$$

Under the deterministic evolution (A9) \mathcal{M} and ϕ have trivial dynamics $\dot{\mathcal{M}} = 0$ and $\dot{\phi} = |\Omega|$. Using Ito calculus we derive the exact stochastic equation for \mathcal{M}

$$d\mathcal{M} = a(\mathcal{M}, \phi)dt + \sum_i b_i(\mathcal{M}, \phi)dW_i, \quad (\text{A14})$$

where dW_i reflect the real and imaginary parts of $d\xi_{\alpha}$. We avoid providing the long analytical expressions for a and b_i . Since \mathcal{M} is a constant of the deterministic motion, a and b_i originate from the noise terms in Eq. (A8) and thus come with a prefactor $\frac{\kappa}{j}$, which sets the time scale of “torus hopping,” i.e., evolution of \mathcal{M} , much larger than the time scale of the evolution of the angle ϕ . Thus we can average over the fast ϕ , as in [25,34,35],

$$d\mathcal{M} = \langle a(\mathcal{M}, \phi) \rangle_{\phi} dt + \sum_i \sqrt{\langle b_i^2(\mathcal{M}, \phi) \rangle_{\phi}} dW_i, \quad (\text{A15})$$

$$\langle \dots \rangle_{\phi} = \frac{1}{2\pi} \int_0^{2\pi} d\phi (\dots),$$

and obtain a one-dimensional equation for \mathcal{M} . For a one-dimensional Ito equation the steady-state distribution can always be found analytically. We obtain

$$P(\mathcal{M}) = \frac{1}{2} \frac{\sqrt{1+2\lambda^2}}{\tanh^{-1}((1+2\lambda^2)^{-1/2})} \frac{1}{2\lambda^2 + 1 - \mathcal{M}^2}, \quad (\text{A16})$$

which defines the following steady state for large (but finite) j :

$$\rho_{ss} = \int_{-1}^1 d\mathcal{M} P(\mathcal{M}) \int_0^{2\pi} d\phi \frac{1}{2\pi} |\mu(\mathcal{M}, \phi)\rangle \langle \mu(\mathcal{M}, \phi)|. \quad (\text{A17})$$

The J_z variance of a single torus is dependent on the torus label \mathcal{M} and given by

$$\langle J_z^2(\mathcal{M}) \rangle = \frac{1}{2\pi} \int_0^{2\pi} d\phi \langle \mu(\mathcal{M}, \phi) | J_z^2 | \mu(\mathcal{M}, \phi) \rangle$$

$$= \frac{j^2}{2} (\lambda^2 - 1) \left(\frac{\lambda}{\sqrt{\lambda^2 - (1 - \mathcal{M}^2)}} - 1 \right). \quad (\text{A18})$$

For a fixed $\mathcal{M} \neq 0$, each variance follows a simple power law (exponent one) as $\lambda = 1 + \varepsilon \rightarrow 1^+$:

$$\frac{\langle J_z^2(\mathcal{M}) \rangle}{j^2} = \frac{1 - |\mathcal{M}|}{|\mathcal{M}|} \varepsilon + O(\varepsilon^2). \quad (\text{A19})$$

Note, however, the singular prefactor as $\mathcal{M} \rightarrow 0$. Indeed, the case $\mathcal{M} = 0$ is special as the corresponding torus does not break the mirror symmetry of the GKSL master equation (1) of the main text (mirror reflections set $\mathcal{M} \rightarrow -\mathcal{M}$). We find for $\varepsilon \rightarrow 0^+$ the square root behavior

$$\frac{\langle J_z^2(\mathcal{M} = 0) \rangle}{j^2} = \frac{\varepsilon^{\frac{1}{2}}}{\sqrt{2}} + O(\varepsilon). \quad (\text{A20})$$

The true steady state (A17) for any finite but large j , however, features a mixture of these behaviors: from (A16), (A17), and (A18) we can compute the J_z variance of ρ_{SS} just by averaging over the distribution of tori and obtain

$$\begin{aligned} \frac{\langle J_z^2 \rangle}{j^2} &= \int_{-1}^1 d\mathcal{M} P(\mathcal{M}) \frac{\langle J_z^2(\mathcal{M}) \rangle}{j^2} \\ &= (\lambda^2 - 1) \left(\frac{\tanh^{-1}(\sqrt{3}(1 + 2\lambda^2)^{-1/2})}{\sqrt{3} \tanh^{-1}((1 + 2\lambda^2)^{-1/2})} - 1 \right). \end{aligned} \quad (\text{A21})$$

For very large j the timescale separation of the hopping process and the deterministic cyclic evolution is perfect. Thus

the result is the exact asymptotic curve in Fig. 4. Close to the transition $\lambda = 1 + \varepsilon$ this curve does not behave like a power law. We find the expansion

$$\frac{\langle J_z^2 \rangle}{j^2} = \frac{-\varepsilon \ln \varepsilon + \varepsilon (\ln 3 - 2\sqrt{3} \tanh^{-1}(\sqrt{3}^{-1})) + O(\varepsilon^2)}{\sqrt{3} \tanh^{-1}(\sqrt{3}^{-1})}. \quad (\text{A22})$$

Trying to establish an “exponent” $\beta(\varepsilon) = \frac{\partial(\ln(\dots))}{\partial(\ln(\varepsilon))}$ for the variance $\frac{\langle J_z^2 \rangle}{j^2}$ leads to the peculiar behavior $\beta(\varepsilon) = 1 + \frac{1}{\ln \varepsilon} + \dots$ as $\varepsilon \rightarrow 0^+$, with $\beta(0) = 1$ and an infinite negative initial slope $\beta'(\varepsilon) = -\frac{1}{\varepsilon \ln(\varepsilon)^2}$ in the limit $\varepsilon \rightarrow 0^+$, as is apparent in Fig. 4(b).

-
- [1] R. H. Dicke, *Phys. Rev.* **93**, 99 (1954).
 - [2] F. Dimer, B. Estienne, A. S. Parkins, and H. J. Carmichael, *Phys. Rev. A* **75**, 013804 (2007).
 - [3] E. G. Dalla Torre, S. Diehl, M. D. Lukin, S. Sachdev, and P. Strack, *Phys. Rev. A* **87**, 023831 (2013).
 - [4] R. Gutiérrez-Jáuregui and H. J. Carmichael, *Phys. Rev. A* **98**, 023804 (2018).
 - [5] M.-J. Hwang, P. Rabl, and M. B. Plenio, *Phys. Rev. A* **97**, 013825 (2018).
 - [6] K. Baumann, C. Guerlin, F. Brennecke, and T. Esslinger, *Nature (London)* **464**, 1301 (2010).
 - [7] M. Greiner, O. Mandel, T. Esslinger, T. W. Hänsch, and I. Bloch, *Nature (London)* **415**, 39 (2002).
 - [8] A. M. Shakirov, Y. E. Shchadilova, A. N. Rubtsov, and P. Ribeiro, *Phys. Rev. B* **94**, 224425 (2016).
 - [9] J. S. Ferreira and P. Ribeiro, *arXiv:1801.00818*.
 - [10] P. Ribeiro and T. Prosen, *Phys. Rev. Lett.* **122**, 010401 (2019).
 - [11] L. M. Sieberer, M. Buchhold, and S. Diehl, *Rep. Prog. Phys.* **79**, 096001 (2016).
 - [12] L. M. Sieberer, A. Chiocchetta, A. Gambassi, U. C. Täuber, and S. Diehl, *Phys. Rev. B* **92**, 134307 (2015).
 - [13] J. Raftery, D. Sadri, S. Schmidt, H. E. Türeci, and A. A. Houck, *Phys. Rev. X* **4**, 031043 (2014).
 - [14] J. Hannukainen and J. Larson, *Phys. Rev. A* **98**, 042113 (2018).
 - [15] D. Nagy and P. Domokos, *Phys. Rev. Lett.* **115**, 043601 (2015).
 - [16] E. G. Dalla Torre, E. Demler, T. Giamarchi, and E. Altman, *Nat. Phys.* **6**, 806 (2010).
 - [17] J. Gelhausen and M. Buchhold, *Phys. Rev. A* **97**, 023807 (2018).
 - [18] V. Gorini, A. Kossakowski, and E. C. G. Sudarshan, *J. Math. Phys.* **17**, 821 (1976); G. Lindblad, *Commun. Math. Phys.* **48**, 119 (1976).
 - [19] W. T. Strunz, *J. Phys. A: Math. Gen.* **30**, 4053 (1997).
 - [20] N. Gisin and I. C. Percival, *J. Phys. A: Math. Gen.* **25**, 5677 (1992).
 - [21] M. B. Plenio and P. L. Knight, *Rev. Mod. Phys.* **70**, 101 (1998).
 - [22] W. T. Strunz and I. C. Percival, *J. Phys. A: Math. Gen.* **31**, 1801 (1998).
 - [23] D. F. Walls, P. D. Drummond, S. S. Hassan, and H. J. Carmichael, *Prog. Theor. Phys. Suppl.* **64**, 307 (1978).
 - [24] D. F. Walls, *J. Phys. B* **13**, 2001 (1980).
 - [25] P. Drummond and H. Carmichael, *Opt. Commun.* **27**, 160 (1978).
 - [26] F. Iemini, A. Russomanno, J. Keeling, M. Schirò, M. Dalmonte, and R. Fazio, *Phys. Rev. Lett.* **121**, 035301 (2018).
 - [27] S. Morrison and A. S. Parkins, *J. Phys. B* **41**, 195502 (2008).
 - [28] S. Schneider and G. J. Milburn, *Phys. Rev. A* **65**, 042107 (2002).
 - [29] N. Shammah, S. Ahmed, N. Lambert, S. De Liberato, and F. Nori, *Phys. Rev. A* **98**, 063815 (2018).
 - [30] K. Tucker, B. Zhu, R. J. Lewis-Swan, J. Marino, F. Jimenez, J. G. Restrepo, and A. M. Rey, *New J. Phys.* **20**, 123003 (2018).
 - [31] N. Gisin and M. B. Cilibs, *J. Phys. A: Math. Gen.* **25**, 5165 (1992).
 - [32] W. T. Strunz, in *Coherent Evolution in Noisy Environments*, edited by A. Buchleitner and K. Hornberger (Springer, Berlin, Heidelberg, 2008).
 - [33] The mirror reflected state to a coherent state $|\mu\rangle$ is $|\mu^*\rangle$.
 - [34] H. J. Carmichael, *J. Phys. B* **13**, 3551 (1980).
 - [35] A. Kruscha, R. Ketzmerick, and H. Kantz, *Phys. Rev. E* **85**, 066210 (2012).
 - [36] Ito noise increments scale as $d\xi \rightarrow \sqrt{a} d\xi$.